PD-like Regulation of Mechanical Systems with Prescribed Bounds of Exponential Stability: the Point-to-Point Case

Davide Calzolari[1], Cosimo Della Santina[1,2], *Member, IEEE*, and Alin Albu-Schäffer[1], *Fellow, IEEE*

***Abstract*—This letter discusses an extension of the famous PD regulator implementing point to point motions with prescribed exponential rates of convergence. This is achieved by deriving a novel global exponential stability result, dealing with mechanical systems evolving on uni-dimensional invariant manifolds of the configuration space. The construction of closed loop controllers enforcing the existence of such manifolds is then discussed. Explicit upper and lower bounds of convergence are provided, and connected to the gains of the closed loop controller. Simulations are carried out, assessing the effectiveness of the controller and the tightness of the exponential bounds.**

***Index Terms*—PID control; Robotics; Lyapunov methods**

I. Introduction

Proving and quantifying exponential convergence of a system to an equilibrium are important steps in characterizing its transient and asymptotic behavior [1, Sec. 1.3]. Yet, despite the practical importance of the matter, this challenge has never been fully tackled for nonlinear mechanical systems. Consider for example a smooth mechanical system with n Degrees of Freedom (DoF), and configuration dependent and bounded [2] inertia tensor, as the one shown in Fig. 1. Such a system can be described by a set of n second order ordinary differential equations [3]

$$\boldsymbol{M}(\boldsymbol{q})\ddot{\boldsymbol{q}} + \boldsymbol{C}(\boldsymbol{q},\dot{\boldsymbol{q}})\dot{\boldsymbol{q}} = \boldsymbol{\tau}(\boldsymbol{q},\dot{\boldsymbol{q}}), \tag{1}$$

where $\boldsymbol{q},\dot{\boldsymbol{q}},\ddot{\boldsymbol{q}} \in \mathbb{R}^n$ is the configuration vector with its time derivatives. The matrix $\boldsymbol{M}(\boldsymbol{q}) \in \mathbb{R}^{n\times n}$ is the inertia tensor, and $\boldsymbol{C}(\boldsymbol{q},\dot{\boldsymbol{q}})\dot{\boldsymbol{q}}$ collects Coriolis and centrifugal forces. Finally, $\boldsymbol{\tau}(\boldsymbol{q},\dot{\boldsymbol{q}})$ is a generic set of generalized forces which can include any combination of feedback actions, conservative forces, and friction induced dissipative forces.

Quantitative convergence results can be provided when strong model compensations are imposed, as for example when using computed torque control. Indeed, the effect of this established technique is to match the nonlinear dynamics to a linear one, where exponential rate can be explicitly evaluated. We are interested here instead in the case in which

$$\boldsymbol{\tau}(\boldsymbol{q},\dot{\boldsymbol{q}}) = \boldsymbol{P}(\boldsymbol{q}) + \boldsymbol{D}(\boldsymbol{q})\dot{\boldsymbol{q}}. \tag{2}$$

This can either represent a mechanical impedance (if $\boldsymbol{P}$ is a potential and $\boldsymbol{D}$ is positive definite damping), a nonlinear Proportional Derivative (PD) controller or a combination of the two. This is a relevant choice since PD controllers are still very popular control approach in the practice [4], and a quite active topic of research [5]–[7].

[1] The authors are with the Department of Informatics, Technical University of Munich (TUM), 85748 Garching, Germany, and with the Institute of Robotics and Mechatronics, German Aerospace Center (DLR), 82234 Weßling, Germany davide.calzolari@dlr.de

[2] The author is with the Cognitive Robotics Department, Delft University of Technology (TU Delft), Delft, The Netherlands.

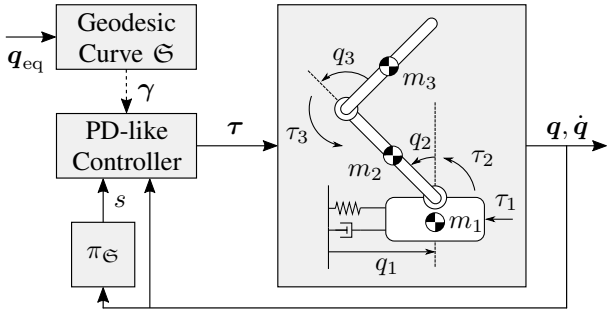

Figure 1. We propose a PD controller implementing exponentially fast point-to-point motions. The key idea is to generate the control action such that it is always tangent to the geodesics curve - induced by the inertia tensor metrics - connecting the starting and the ending point. The strategy is tested in simulation on a double pendulum connected to a cart.

The usual convergence analyses [8] employ the total energy of the system as (control) Lyapunov candidate. Yet, this is not a strict Lyapunov function [1], and it cannot be used to assess exponential convergence. Several works over the years have solved this issue for very specific choices of (1) and (2). These efforts are well reviewed in [9]. Moving to a more general setting, one popular way of circumventing the problem is skewing the virtual energy by adding an infinitesimal term $\epsilon\dot{\boldsymbol{q}}^T\boldsymbol{M}(\boldsymbol{q})\boldsymbol{q}$. The resulting candidate is a strict Lyapunov function for small enough ϵ [3, Sec. 5.3], due to the sign indefiniteness of $\boldsymbol{C}(\boldsymbol{q},\dot{\boldsymbol{q}})$. Despite its theoretical relevance, this result has limited practical use, since it provides convergence rates which are arbitrarily close to zero, and therefore a poor estimation of the empirical convergence rates evaluated by Monte-Carlo simulations or by experiments. An alternative approach [10]–[12] is to impose high lower bounds on the norms of $\boldsymbol{P}$ and $\boldsymbol{D}$, so that the effect of (2) is dominant with respect to the left hand side of (1), i.e., the rigid body dynamics. As a result, very high gains are needed to produce meaningful convergence rates, often preventing the practical applicability of the method.

We moved a first step towards a general solution to the problem in [13], where we tackled the case $n = 1$. The idea is here to introduce an energy-based change of coordinates which makes $\boldsymbol{C}(\boldsymbol{q},\dot{\boldsymbol{q}})$ disappear, solving therefore the problem of its sign indefiniteness. The present work moves from this initial effort, venturing into the world of n degrees of freedom. More specifically the present paper contributes to the state of the art of control of mechanical systems with

- tight and analytical bounds of convergence for a system in the general form (1), (2), *when evolving on a one dimensional sub-manifold of the configuration space with line topology*;
- conditions for such a manifold to exist, and how to design a feedback controller enforcing its existence;

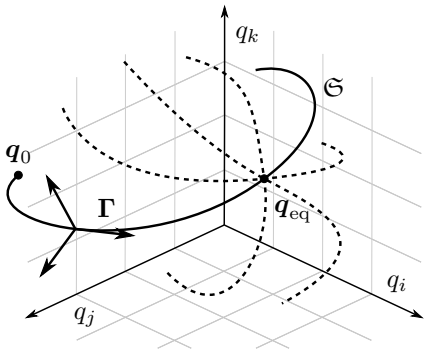

Figure 2. Given an initial configuration $\boldsymbol{q}_0$ and the equilibrium $\boldsymbol{q}_{\text{eq}}$ in $\mathbb{R}^n$, there is always a geodesic curve $\mathfrak{S}$ connecting them. Any control law $\tau(q,\dot{q})$ satisfying (5) enforces the trajectories to evolve along this one dimensional manifold without the need to cancel Coriolis/centrifugal forces. As a consequence, it allows to analyze the stability properties of the n-DoF system by looking at a simple scalar system.

- a nonlinear PD controller, which generates *point to point motions with prescribed rate of convergence*, without the need of using high gains and without requiring the cancellation of the gyroscopic forces.

II. Preliminaries

An embedded sub-manifold of the system configuration space $\mathfrak{S} \subset \mathbb{R}^n$ is invariant if

$$\forall \boldsymbol{q}(0) \in \mathfrak{S},\ \dot{\boldsymbol{q}}(0) \in T_{\boldsymbol{q}(0)}\mathfrak{S} \Rightarrow \boldsymbol{q}(t) \in \mathfrak{S},\ \forall t, \tag{3}$$

where $T_{\boldsymbol{q}(0)}\mathfrak{S}$ is the tangent space of $\mathfrak{S}$ in $\boldsymbol{q}(0)$. We consider here line-shaped manifolds, i.e., we assume the existence of a continuous function $\boldsymbol{\gamma} : \mathbb{R} \to \mathfrak{S}$ which is invertible with continuous inverse (i.e., an homeomorphism). Therefore, the state of the mechanical system evolving in $\mathfrak{S}$ can always be expressed as

$$\boldsymbol{q} = \boldsymbol{\gamma}(s), \quad \dot{\boldsymbol{q}} = \frac{\partial \boldsymbol{\gamma}(s)}{\partial s}\dot{s} = \boldsymbol{\Gamma}(s)\dot{s}, \tag{4}$$

where s is a parametrization of $\boldsymbol{\gamma}$. Note that $\boldsymbol{\Gamma}$ is always full rank by definition of $\boldsymbol{\gamma}$. We call $\boldsymbol{q}_{\text{eq}}$ the equilibrium that we aim at stabilizing, i.e., we take $\boldsymbol{\tau}(\boldsymbol{q}_{\text{eq}}, 0) = 0$, where $\boldsymbol{q}_{\text{eq}} \in \mathfrak{S}$. We will show in the next section that this is without loss of generality. We define the low-dimensional parametrization of the equilibrium as s_{eq} such that $\boldsymbol{q}_{\text{eq}} = \boldsymbol{\gamma}(s_{\text{eq}})$.

III. Existence and Feedback Enforcement of $\mathfrak{S}$

A valid tool for realizing the invariant manifold $\mathfrak{S}$ is feedback based enforcing of the virtual holonomic constraints $\boldsymbol{\gamma}(\pi_{\mathfrak{S}}(\boldsymbol{q})) = \boldsymbol{q}$, where $\pi_{\mathfrak{S}}$ is a projection of $\mathbb{R}^n$ in $\mathfrak{S}$. This can be done using the techniques discussed in [14], [15]. This solution is however projection dependent, and can potentially encompass a strong component of model compensation not coherent with (2).

We consider here an alternative coherent with a PD-like action, and that results from a generalization of the so-called strict mode concept introduced in [16], [17]. Suppose that $\mathfrak{S}$ exists with $\boldsymbol{\tau} = \partial U/\partial \boldsymbol{q} + \boldsymbol{D}(\boldsymbol{q})\dot{\boldsymbol{q}}$, for some potential energy $U : \mathbb{R} \to \mathbb{R}$ and nonlinear damping $\boldsymbol{D} \succeq 0$. In this case the manifold is called strict mode, since it can be seen as the generalization of a linear eigenspaces to a general non-Euclidean setting (refer to [17] for a complete discussion on the topic). The following Lemma introduces a generalization of the existence result provided in [16] to the general case (1). Note indeed that in [16] the action $\boldsymbol{\tau}(\boldsymbol{q}, \dot{\boldsymbol{q}})$ is an integrable potential field. We consider here the general case instead.

Lemma 1. *Sufficient conditions for the manifold $\mathfrak{S}$ with parameterization $\boldsymbol{\gamma}(s)$ to exist for system* (1) *are*

- *an $f : \mathbb{R}^2 \to \mathbb{R}$ exists such that the on-manifold value of the torque is*

$$[\boldsymbol{\tau}(\boldsymbol{q}, \dot{\boldsymbol{q}})]_{\boldsymbol{q}=\boldsymbol{\gamma}(s), \dot{\boldsymbol{q}}=\boldsymbol{\Gamma}(s)\dot{s}} = \boldsymbol{M}(\boldsymbol{\gamma}(s))\boldsymbol{\Gamma}(s) f(s, \dot{s}) , \tag{5}$$

- *a time evolution $\sigma : \mathbb{R} \to \mathbb{R}$ exists such that $(\boldsymbol{q}, \dot{\boldsymbol{q}}) = (\boldsymbol{\gamma}(\sigma), \boldsymbol{\Gamma}(\sigma)\dot{\sigma})$ is a solution of*

$$\boldsymbol{M}(\boldsymbol{q})\ddot{\boldsymbol{q}} + \boldsymbol{C}(\boldsymbol{q}, \dot{\boldsymbol{q}})\dot{\boldsymbol{q}} = \boldsymbol{0} . \tag{6}$$

In other words $\boldsymbol{\gamma}$ identifies a geodesic curve for the metric induced by the tensor $\boldsymbol{M}(\boldsymbol{q})$.

Proof. Consider $\mathfrak{S}$ a geodesic curve for the metric induced by the tensor $\boldsymbol{M}(\boldsymbol{q})$, with $\boldsymbol{\Gamma}$ defined as in (4). Substituting (5) in (1) and pre-multiplying by $\boldsymbol{M}^{-1}$ yields

$$\ddot{\boldsymbol{q}} + \boldsymbol{M}^{-1}\boldsymbol{C}\dot{\boldsymbol{q}} = \boldsymbol{\Gamma} f . \tag{7}$$

Let us introduce a local set of coordinates $\boldsymbol{\xi} \in \mathbb{R}^{n-1}$ in the directions orthogonal to $\mathfrak{S}$ such that the configuration $\boldsymbol{q}$ can be expressed using a a local diffeomorphism $h : \mathrm{R}^n \to \mathrm{R}^n$ between $(s, \boldsymbol{\xi})$ and $\boldsymbol{q}$ as

$$h(s, \boldsymbol{\xi}) = \boldsymbol{\gamma}(s) + \boldsymbol{\Gamma}_{\perp}(s)\boldsymbol{\xi} . \tag{8}$$

Differentiating (8) with respect to time yields

$$\dot{\boldsymbol{q}} = \begin{bmatrix}\boldsymbol{\Gamma} & \boldsymbol{\Gamma}_{\perp}\end{bmatrix}\begin{bmatrix}\dot{s} \\ \dot{\boldsymbol{\xi}}\end{bmatrix} + \dot{\boldsymbol{\Gamma}}_{\perp}\boldsymbol{\xi} = \boldsymbol{H}\begin{bmatrix}\dot{s} \\ \dot{\boldsymbol{\xi}}\end{bmatrix} + \dot{\boldsymbol{\Gamma}}_{\perp}\boldsymbol{\xi} , \tag{9}$$

$$\ddot{\boldsymbol{q}} = \boldsymbol{H}\begin{bmatrix}\ddot{s} \\ \ddot{\boldsymbol{\xi}}\end{bmatrix} + \dot{\boldsymbol{H}}\begin{bmatrix}\dot{s} \\ \dot{\boldsymbol{\xi}}\end{bmatrix} + \dot{\boldsymbol{\Gamma}}_{\perp}\dot{\boldsymbol{\xi}} + \ddot{\boldsymbol{\Gamma}}_{\perp}\boldsymbol{\xi} . \tag{10}$$

where $\boldsymbol{\Gamma}^T\boldsymbol{\Gamma}_{\perp} = \boldsymbol{0}$ by construction. We can now express the dynamics (7) using $(s, \boldsymbol{\xi})$ coordinates by substituting (8), (9), and (10), and pre-multiplying by $\boldsymbol{H}^T$, yielding

$$\begin{bmatrix}H_s & \boldsymbol{0} \\ \boldsymbol{0} & \boldsymbol{H}_{\xi}\end{bmatrix}\begin{bmatrix}\ddot{s} \\ \ddot{\boldsymbol{\xi}}\end{bmatrix} + \boldsymbol{\mu}\begin{bmatrix}\dot{s} \\ \dot{\boldsymbol{\xi}}\end{bmatrix} + \dot{\boldsymbol{\Gamma}}_{\perp}\dot{\boldsymbol{\xi}} + \boldsymbol{A}\boldsymbol{\xi} = \begin{bmatrix}H_s \\ \boldsymbol{0}\end{bmatrix} f , \tag{11}$$

where

$$\boldsymbol{\mu} = \begin{bmatrix}\mu_s & \boldsymbol{\mu}_{s,\xi} \\ \boldsymbol{\mu}_{\xi,s} & \boldsymbol{\mu}_{\xi}\end{bmatrix} = \boldsymbol{H}^T\left(\dot{\boldsymbol{H}} + \boldsymbol{M}^{-1}\boldsymbol{C}\boldsymbol{H}\right) ,$$
$$\boldsymbol{A} = \boldsymbol{H}^T\left(\boldsymbol{M}^{-1}\boldsymbol{C}\dot{\boldsymbol{\Gamma}}_{\perp} + \ddot{\boldsymbol{\Gamma}}_{\perp}\right) .$$

Consider now the case where $\boldsymbol{\xi}(0) = \dot{\boldsymbol{\xi}}(0) = \boldsymbol{0}$, i.e., the system is initially on $\mathfrak{S}$, and no input forces are present, i.e., $f = 0$: since $\mathfrak{S}$ is a geodesic, the system naturally evolves on $\mathfrak{S}$, thus it must hold $\boldsymbol{\xi}(t) = \dot{\boldsymbol{\xi}}(t) = \ddot{\boldsymbol{\xi}}(t) = \boldsymbol{0}, \forall t \geq 0$. This imposes the following constraint on the dynamics of $\boldsymbol{\xi}$

$$\boldsymbol{\mu}_{\xi,s}\dot{s} = \boldsymbol{0}, \quad \forall t \geq 0 , \tag{12}$$

which implies that $\boldsymbol{\mu}_{\xi,s}$ must remain zero along a geodesic. This reflects the well-known fact that, on a geodesic, the gyroscopic forces are purely tangential to the curve. Since the control action defined by (5) acts solely on the first equation of (11), the dynamics of $\boldsymbol{\xi}$ remains decoupled, hence, given the initial condition $\boldsymbol{q}(0) \in \mathfrak{S}, \dot{\boldsymbol{q}}(0) \in T_{q(0)}\mathfrak{S}$, then the manifold $\mathfrak{S}$ is invariant. □

Note that these conditions become also necessary in case $\mathfrak{S}$ is required to be a strict mode, i.e., if we ask $\boldsymbol{\tau}$ to be fully implementable by mechanical components. The conservative case $\boldsymbol{D} = 0$ is proven in [16], and the general case follows from similar arguments.

The following Corollary of Lemma 1 proves that this control action is a good candidate for achieving point-to-point control.

Corollary 1. *For all $\dot{\boldsymbol{q}}(0) = 0$ then a $\boldsymbol{\tau}$ verifying Lemma 1 can be selected such that the closed loop admits a $\mathfrak{S}$ with $\boldsymbol{q}(0) \in \mathfrak{S}$ and $\boldsymbol{q}_{\rm eq} \in \mathfrak{S}$.*

Proof. The thesis directly follows by the fact that a geodesics always exists connecting any two configurations of (1) - by the very definition [18] of geodesic curve $\boldsymbol{\gamma}$. □

Therefore our analysis can be seen as a quasi-global one, in the sense that the entire configuration space can be analyzed with the proposed tools since every admissible configuration can be connected to the equilibrium $\boldsymbol{q}_{\rm eq}$ - as the configuration space $\mathbb{R}^n$ is simply connected. Note that such geodesic can be evaluated through standard methods in computational geometry, see for example [19].

In the following we consider among all the possible $\boldsymbol{\tau}$ verifying (5), the PD-like controller

$$\boldsymbol{\tau} = -\boldsymbol{M}(\boldsymbol{q})\left[\kappa(s)\boldsymbol{\Gamma}(s)(s - s_{\rm eq}) + \delta(s)\dot{\boldsymbol{q}}\right], \quad s = \pi_{\mathfrak{S}}(\boldsymbol{q}), \quad (13)$$

where $\pi_{\mathfrak{S}}$ is a projection from $\mathbb{R}^n$ to $\mathfrak{S}$, i.e. any function such that $\pi_{\mathfrak{S}} \circ \boldsymbol{\gamma}$ is the identity, and $\kappa(s), \delta(s)$ are positive definite scalar functions. It is immediate to see that (13) verifies (5) for $\boldsymbol{q} \in \mathfrak{S}$ considering $f(s, \dot{s}) = -\kappa(s)(s - s_{\rm eq}) - \delta(s)\dot{s}$, and in view of (4). It is worthy to remark that, in contrast to computed torque control, which forces the evolution along paths which minimize the Euclidean distance, the proposed controller drives the system along geodesics that optimally minimize the kinetic energy difference when traveling between configurations. As a result, (13) does not cancel the gyroscopic forces, leading to a passive controller and higher efficiency.

Note that geodesics - there induced by non-inertial metrics - have been used in combination to PD controllers already in [20, Ch. 11]. However, the aim is there to define the error signal in a coordinate-free way, rather than to exploit some property of the system when evolving on a geodesic.

IV. Convergence Results

A. Dynamics along $\mathfrak{S}$

We aim here at writing a compact description of the mechanical system dynamics when evolving on the manifold thanks to the action (13). To this end we differentiate once $\dot{q}$ from (4), yielding

$$\ddot{\boldsymbol{q}} = \boldsymbol{\Gamma}(s)\ddot{s} + \dot{\boldsymbol{\Gamma}}(s, \dot{s})\dot{s} \, . \quad (14)$$

Pre-multiply both sides of the equation for $\boldsymbol{\Gamma}^T\boldsymbol{M}$ gets to

$$\left(\boldsymbol{\Gamma}^T\boldsymbol{M}\boldsymbol{\Gamma}\right)\ddot{s} = \boldsymbol{\Gamma}^T\left(\boldsymbol{M}\ddot{\boldsymbol{q}}\right) - \boldsymbol{\Gamma}^T\boldsymbol{M}\dot{\boldsymbol{\Gamma}}\dot{s}. \quad (15)$$

Finally, we substitute the expression of $\boldsymbol{M}\ddot{\boldsymbol{q}}$ from (1), and $\boldsymbol{q}, \dot{\boldsymbol{q}}$ from (4), resulting in the following on-manifold dynamics

$$m(s)\ddot{s} + c(s, \dot{s})\dot{s} + k(s)s + d(s)\dot{s} = 0 \, , \quad (16)$$

where we assume $s_{\rm eq} = 0$ without loss of generality, and

$$m(s) = \boldsymbol{\Gamma}^T\boldsymbol{M}\boldsymbol{\Gamma} \, , \quad c(s, \dot{s}) = \boldsymbol{\Gamma}^T\boldsymbol{C}\boldsymbol{\Gamma} - \boldsymbol{\Gamma}^T\dot{\boldsymbol{\Gamma}} \, , \quad (17)$$

$$k(s) = \kappa(s)\boldsymbol{\Gamma}^T\boldsymbol{M}\boldsymbol{\Gamma} = \kappa(s)m(s) \, , \quad (18)$$

$$d(s) = \delta(s)\boldsymbol{\Gamma}^T\boldsymbol{M}\boldsymbol{\Gamma} = \delta(s)m(s) \, . \quad (19)$$

Note that this is equivalent to a one dimensional mechanical system with configuration dependent inertia, which is similar to the one we studied in [13], albeit with a more general nonlinear impedance. Therefore, the results that we introduce in the following can be applied to one dimensional systems with configuration dependent inertia as special case.

B. Properties

Since $\boldsymbol{M}$ is bounded [2] and (17) is a tensor transformation with $\boldsymbol{\Gamma}(s)$ bounded, it results

$$\underline{m} \leq m(s) \leq \overline{m} \, , \quad (20)$$

with $\underline{m} > 0$. Moreover, we assume that

$$\underline{k} \leq k(s) \, , \quad (21)$$

$$\underline{d} \leq d(s) \leq \overline{d} \, , \quad (22)$$

with $\underline{k}, \underline{d} > 0$. Furthermore, the following well-known property of mechanical systems [3] is maintained

$$\dot{m}(s, \dot{s}) = 2c(s, \dot{s}) \, . \quad (23)$$

C. Coordinates change

Consider the following coordinate transformation

$$\psi = \sqrt{\frac{m(s)}{2}}\dot{s}, \quad \varphi = \sqrt{\frac{1}{2}}s, \quad (24)$$

where ψ is the signed square root of the kinetic energy, while φ is a scaling of q. In the new coordinates, system (16) can be re-written as

$$\dot{\psi} = -\frac{d(s)}{m(s)}\psi - \frac{k(s)}{\sqrt{m(s)}}\varphi \, , \qquad \dot{\varphi} = \frac{1}{\sqrt{m(s)}}\psi \, , \quad (25)$$

where (23) and the inverse coordinate transformation have been used. We leave for now explicit the dependence on the configuration s of m, d, and k. The gyroscopic term along the geodesic vanishes, without any need of explicit compensation.

D. Two skewed Lyapunov candidates

We define the following Lyapunov function candidates, with the objective of tightly bounding the convergence rate of (16). To study the upper bound we consider

$$V_u(\psi, \varphi) = \begin{bmatrix}\psi & \varphi\end{bmatrix}\boldsymbol{P}_u(s)\begin{bmatrix}\psi \\ \varphi\end{bmatrix} \, , \quad (26)$$

where

$$\boldsymbol{P}_u = \begin{bmatrix}1 & \xi_u \\ \xi_u & \alpha(s)\end{bmatrix}, \quad \xi_u = \frac{\underline{d}}{2\eta_u\sqrt{\overline{m}}}, \quad \alpha(s) = \frac{2\int_0^s k(y)y \, dy}{s^2}. \quad (27)$$

Here, ξ_u is a constant, with $\eta_u \geq 1$, while $\alpha(s)$ depends on the configuration s and it can be interpreted as a generalization of the role that the stiffness has in the linear case within the potential field. Moreover, in [13] it was shown that

$$\alpha(s) \geq \underline{k} \, . \quad (28)$$

To analyze the lower bound we consider

$$V_l(\psi,\varphi) = \begin{bmatrix}\psi & \varphi\end{bmatrix} \boldsymbol{P}_l(s) \begin{bmatrix}\psi \\ \varphi\end{bmatrix} , \tag{29}$$

where

$$\boldsymbol{P}_l = \begin{bmatrix}1 & \xi_l \\ \xi_l & \alpha(s)\end{bmatrix} , \quad \xi_l = \frac{\overline{d}}{2\eta_l\sqrt{\underline{m}}} , \tag{30}$$

with $\eta_l \geq 1$.

Remark 1. *Since $\alpha(s)$ is positive and lower bounded, it is always possible to properly define* (26) *and* (29) *by taking η_u and η_l large enough.*

Let us define the quantities

$$\beta_m = \min_{s\in\mathfrak{S}} \frac{k(s)}{\alpha(s)}, \quad \beta_M = \max_{s\in\mathfrak{S}} \frac{k(s)}{\alpha(s)} ,$$

then, the following inequalities trivially hold

$$-k(s) \leq -\beta_m\alpha(s) , \quad 0 < \beta_m \leq 1 , \tag{31}$$

$$-k(s) \geq -\beta_M\alpha(s) , \quad 1 \leq \beta_M . \tag{32}$$

Lemma 2. *If the conditions*

$$\dot{V}_u \leq -\lambda_u V_u , \tag{33}$$

$$\dot{V}_l \geq -\lambda_l V_l , \tag{34}$$

hold for the Lyapunov function candidates (26) *and* (29)*, then $|| \begin{bmatrix}\psi & \sqrt{\alpha(s)}\varphi\end{bmatrix} ||$ converges exponentially to zero with a rate not lower than $\frac{\lambda_u}{2}$ and not higher than $\frac{\lambda_l}{2}$.*

Proof. The proof can be derived with similar arguments as in [21, Lemma 3.4]. □

E. Bounds on the exponential convergence

The Theorem presented in this section assesses the exponential convergence rates of the n-DoF system implementing (13) and satisfying Lemma 1.

Theorem 1. *System* (16) *converges exponentially to the origin with a rate not lower than*

$$\lambda'_u = \frac{1}{\eta_u}\frac{\beta_m}{\rho}\frac{\underline{d}}{2\overline{m}} , \tag{35}$$

where $\rho > 1$, $\eta_u \geq 1$, if

$$\frac{\underline{d}^2}{4\overline{m}\beta_m\underline{k}} \leq \min_{x\in[\underline{m},\overline{m}]} f_u(x, R_\mathrm{d}) , \tag{36}$$

with f_u defined in (46) *and $R_\mathrm{d} = \overline{d}/\underline{d}$.*

Furthermore, the trajectories converge exponentially with a rate not higher than

$$\lambda'_l = \eta_l\frac{\beta_M}{\theta}\frac{\overline{d}}{2\underline{m}} , \tag{37}$$

where $0 < \theta < 1$, $\eta_l \geq 1$, if

$$\frac{\overline{d}^2}{4\underline{m}\beta_M\underline{k}} \leq \min_{s\in\mathfrak{S}} f_l(m(s), r_\mathrm{D}(s)) , \tag{38}$$

with f_l defined in (48) *and $r_\mathrm{D}(s) = d(s)/\overline{d}$.*

Proof. The derivative of (26) along the system trajectories results in

$$\dot{V}_u(\psi,\varphi) = -\begin{bmatrix}\psi \\ \varphi\end{bmatrix}^T \begin{bmatrix}\frac{2d(s)}{m(s)} - \frac{2\xi_u}{\sqrt{m(s)}}, & \frac{d(s)\xi_u}{m(s)} \\ \frac{d(q)\xi_u}{m(s)}, & \frac{2k(s)\xi_u}{\sqrt{m(s)}}\end{bmatrix} \begin{bmatrix}\psi \\ \varphi\end{bmatrix} . \tag{39}$$

Using (31), equation (39) can be lower bounded as

$$\dot{V}_u(\psi,\varphi) \leq \dot{V}^*_u(\psi,\varphi) = -\begin{bmatrix}\psi \\ \varphi\end{bmatrix}^T \boldsymbol{Q}^*_u(s) \begin{bmatrix}\psi \\ \varphi\end{bmatrix} , \tag{40}$$

where

$$\boldsymbol{Q}^*_u(s) = \begin{bmatrix}\frac{2d(s)}{m(s)} - \frac{2\xi_u}{\sqrt{m(s)}}, & \frac{d(s)\xi_u}{m(s)} \\ \frac{d(s)\xi_u}{m(s)}, & \frac{2\beta_m\alpha(s)\xi_u}{\sqrt{m(s)}}\end{bmatrix} . \tag{41}$$

The exponential convergence rate defined in (35) is implied by imposing that

$$\dot{V}^*_u(\psi,\varphi) \leq -2\lambda'_u V_u(\psi,\varphi) , \tag{42}$$

which is a necessary and sufficient condition for (33) to hold. Combining (26), (40), (42), and (35) yields

$$-\begin{bmatrix}\psi \\ \varphi\end{bmatrix}^T \mathbf{G}_u(s) \begin{bmatrix}\psi \\ \varphi\end{bmatrix} \leq 0 ,$$

where $\mathbf{G}_u(s) = \eta_u\frac{\rho}{\beta_m}\frac{\overline{m}}{\underline{d}}\boldsymbol{Q}^*_u(s) - \boldsymbol{P}_u(s)$. Thus, proving (42) is equivalent to prove that $\mathbf{G}_u(s))$ is positive semi-definite. To this end, we proceed by applying the Sylvester's criterion [22], i.e., we check for positiveness of the determinants of all leading principal minors of $\mathbf{G}_u(s)$

$$G_{u(1,1)} = \frac{\rho\sqrt{\overline{m}}}{\beta_m\sqrt{m(s)}}\left(\frac{2r_d(s)\eta_u\sqrt{\overline{m}}}{\sqrt{m(s)}} - 1\right) - 1 \geq 0 , \tag{43}$$

$$\det(\mathbf{G}_u(s)) \geq 0 , \tag{44}$$

where $r_d(s) = d(s)/\underline{d}$. Inequality (43) is trivially satisfied using (20), (22), and (31). By simplifying and collecting terms, condition (44) can be expressed as

$$f_{u,d}(s)\left(\underline{d}^2\right) + f_{u,k}(s)\left(4\eta_u\overline{m}\beta_m\alpha(s)\right) \leq 0 , \tag{45}$$

where

$$\begin{aligned} f_{u,d}(s) &= \left(\eta_u\rho r_d(s)\overline{m} - \beta_m m(s)\right)^2 , \\ f_{u,k}(s) &= -\eta_u^2\left(m(s) - \rho\sqrt{\overline{m}}\sqrt{m(s)}\right) \\ &\quad \left(\beta_m m(s) - 2\eta_u\rho r_d(s)\overline{m} + \rho\sqrt{\overline{m}}\sqrt{m(s)}\right) . \end{aligned}$$

Provided that

$$\frac{\underline{d}^2}{4\beta_m\alpha(s)\overline{m}} \leq -\frac{f_{u,k}(s)}{f_{u,d}(s)} = f_u(m(s), r_d(s)) , \tag{46}$$

then condition (44) is always verified. Using similar arguments as in [13, Appendix A], it can be shown that the right hand-side of (46) can be lower bounded as

$$\min_{x\in[\underline{m},\overline{m}]} f_u(x, R_d) \leq -\frac{f_{u,k}(s)}{f_{u,d}(s)} . \tag{47}$$

Finally, using (28) to upper bound the left hand-side of (46), and combining it with (47) results into (36), therefore linking this hypothesis to the positive semi-definiteness of $\mathbf{G}_u(s)$, and thus the validity of the exponent λ'_u in (42).

Using similar arguments while imposing (34) for (29), and additionally exploiting (32), it is straightforward to prove the validity of the lower bound λ'_l on the convergence rate defined in (37), provided that the following inequality is satisfied

$$\frac{\overline{d}^2}{4\underline{m}\beta_M\alpha(s)} \leq -\frac{f_{l,k}(s)}{f_{l,d}(s)} = f_l(m(s), r_D(s)) , \tag{48}$$

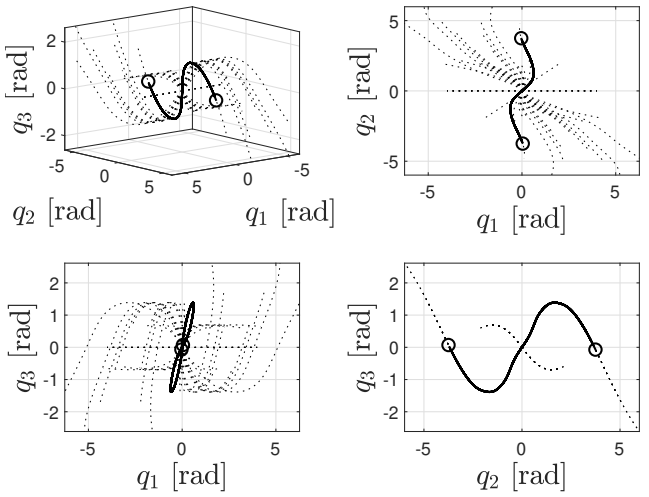

Figure 3. Evolution of the trajectories for system (1) in configuration space during swinging motion (solid line). Thanks to the PD-like control defined in (13), the multi-DoF system evolves on an uni-dimensional manifold, identified with a chosen geodesic curve. Several other geodetic curves crossing the origin are depicted in the figure using dotted lines.

where

$$f_{l,d}(s) = \left(\beta_M \eta_l m(s) - \theta r_D(s)\underline{m}\right)^2 ,$$
$$f_{l,k}(s) = \left(\theta\sqrt{\underline{m}}\sqrt{m(s)} - \eta_l^2 m(s)\right)$$
$$\left(\theta\sqrt{\underline{m}}\sqrt{m(s)} - 2\eta_l\theta r_D(s)\underline{m} + \eta_l^2\beta_M m(s)\right) .$$

Using (28) to upper bound the left hand-side of (48) leads to (38). The thesis follows by the application of Lemma 2.

□

Remark 2. *The total mechanical energy of system* (16) *is*

$$E = || \begin{bmatrix} \psi & \sqrt{\alpha(s)}\varphi \end{bmatrix} ||^2 , \tag{49}$$

thus, Theorem 1 allows to quantitatively estimate the transient behaviour of the energy of system (16) *as well as of system* (1) *using the control defined in* (13)*.*

Remark 3. *Note that the bounds λ_l' and λ_u' are built as by considering the convergence rates of the slowest and fasted frozen systems $\overline{m}\ddot{s} + \underline{d}\dot{s} + \underline{k}s = 0$ and $\underline{m}\ddot{s} + \overline{d}\dot{s} + \underline{k}s = 0$ (i.e., $\underline{d}/2\overline{m}$ and $\overline{d}/2\underline{m}$), relaxed through pre-multiplication for the constants η_l and η_u. If the system is under-damped then the two constants can be taken equal to one.*

Remark 4. *The parameters η_u and η_l can be tuned to trade off the tightness of the convergence rate against the initial size of the bounding envelopes.*

V. Simulations

Let us consider the 3-DoF system depicted in Fig. 1, where $m_1 = m_2 = 1$ [kg], $m_3 = 5$ [kg], $I_{z,2} = 0.1, I_{z,3} = 0.5$ [kg m^2], the links have length 0.5 [m], and the centers of mass of the two links are located at their respective centroid. We use the proposed PD-like action (13) to stabilize the unstable equilibrium (arm straight, pointing upwards), swinging the arm up from its stable one (arm straight, pointing downwards).

The geodesic curve connecting the two can be found by using a simple shooting method, consisting in simulating multiple random initial velocities the dynamics (6). The curve is then parametrized using 25th order polynomials. The resulting shape is shown by Fig. 3.

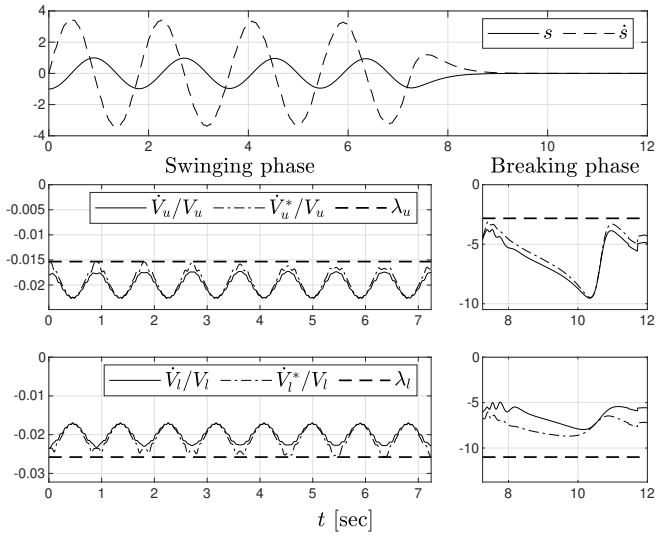

Figure 4. Trajectories of (16) simulated along the chosen geodesic. The bounds on the convergence rates is not over-conservative, as can be seen from the plots of the ratios $\dot{V}_u/V_u$ and $\dot{V}_l/V_l$ against $-\lambda_u$ and $-\lambda_l$, i.e., the upper and lower bounds, respectively.

We aim at assessing the ability of our controller to function both in the under-damped and the over-damped cases, and of our convergence analysis to correctly assess tight convergence bounds in both cases. Therefore, the simulation consists of a swinging phase (slow convergence) followed by a breaking phase (fast convergence).

A. Swinging phase

Initially, the system is commanded to perform a swinging motion using constant gains $\kappa(s) = 12$ and $\delta(s) = 0.02$. The bounds on $m(s), k(s)$ and $d(s)$ are $\underline{m} = 25.94$, $\overline{m} = 31.08$, $\underline{k} = 311.39$, $\underline{d} = 0.52$ and $\overline{d} = 0.62$, while the ratio $\frac{k(s)}{\alpha(s)}$ is bounded by $\beta_m = 0.919$ and $\beta_M = 1.076$. Conditions (36) and (38) are satisfied for $\eta_u = \eta_l = 1, \rho = 1.001$, and $\theta = 0.999$, thus the energy $E = || \begin{bmatrix} \psi & \sqrt{\alpha(s)}\varphi \end{bmatrix} ||^2$ converges exponentially with a minimum rate $\lambda_u = 0.0153$ and a maximum rate $\lambda_l = 0.0258$. The system is simulated starting from the stable equilibrium - which corresponds to $s = -1$ in our parametrization. The resulting trajectories are presented in Fig. 4.

B. Breaking phase

At time $t_b = 7.25$ [sec], the gain $\delta(s)$ is increased such that the energy converges with a desired minimum rate $\lambda_u = 2.75$. To design this gain, a combination of the parameters $\underline{d}, \eta_u$, and ρ must be found such that condition (36) is satisfied for the desired rate. A possible solution is obtained by choosing first $\eta_u = 1.3$ and $\rho = 1.4$, and combining the inequality (36) together with (19), and (22) to solve for δ, leading to the upper bound $\delta(s) \leq 6.77$. Imposing (35) yields the lower bound $\delta(s) \geq 6.53$. Thus, at time t_b, the gain is increased to $\delta(s) = 6.7$, and the system converges to the upstanding equilibrium in a single, well-damped swing, as depicted in Fig. 5. The lower bound on the rate is found using condition

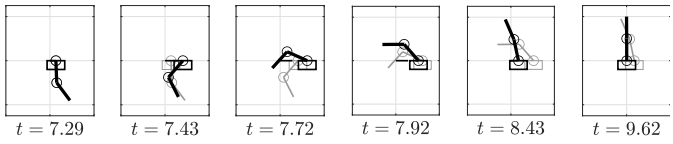

Figure 5. Snapshots of the cart and double pendulum system exponentially converging to the upper equilibrium in a single swing. The gray shape shows the configuration in the previous snapshot.

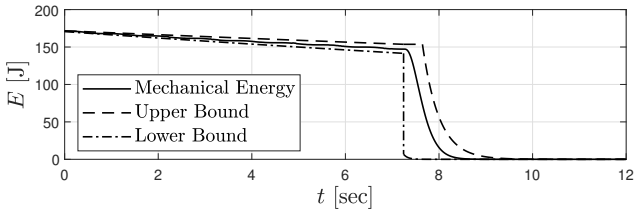

Figure 6. The total mechanical energy of system (1) during the swinging and breaking phases. The upper and lower bounds are evaluated using Theorem 1, and they are depicted in the figure using dashed and dotted lines, respectively.

(38), which is satisfied for $\eta_l = 1.27$. Therefore, the energy is guaranteed to converge exponentially with a minimum rate $\lambda_u = 2.75$ and a maximum rate $\lambda_l = 10.99$.

For both the swinging and breaking phases, plots of the ratios $\dot{V}_u/V_u$ and $\dot{V}_l/V_l$ against the respective bounds are shown in Fig. 4, while the evolution of the energy and the exponential envelopes are depicted in Fig. 6.

Of all the papers discussed in the introduction, the only one that does not fail to produce a convergence rate is [12], which, even so, provides a substantially less tight bound of $\sim$0.16.

C. Comparison with computed torque control

We provide a preliminary comparison of the proposed controller against standard computed torque control (CT) [3, Sec. 5.2]. The initial and final configurations presented for the breaking phase (Fig. 5) are considered for the control task. The gains for CT are matched with the ones used for the PD-like, so to achieve a similar convergence rate. The results of the simulations are depicted in Fig. 7, where the larger torque demands of CT can be acknowledged. Although we suspect that the proposed approach leads to very efficient point-to-point motions, claiming optimality is beyond the scope of the present paper.

VI. Conclusion and Future Work

This work proposed a PD-like controller with prescribed exponential bounds of convergence. For the sake of conciseness, we considered the system to be fully actuated. Nonetheless, we believe that the proposed results can be extended to some classes of under-actuated systems. We will provide such extension in future work. We also aim at understanding if a single closed form proportional action is possible, which substitutes $\boldsymbol{M}(\boldsymbol{q})\boldsymbol{\Gamma}(s)\kappa(s)s$ while covering all the configuration space. Finally, we plan to formally evaluate the robustness of this technique, and validate its effectiveness with experiments on a real system.

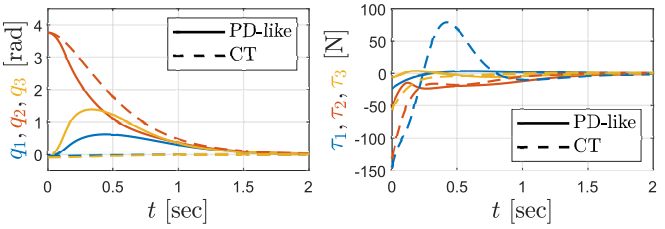

Figure 7. Comparison between the PD-like controller defined in (13) (solid line) and computed torque (dashed line) in terms of convergence of joint trajectories and torque requirements during the point-to-point motion of the breaking phase. The simulations show that the PD-like controller achieves the same convergence rate as CT with a remarkably lower torque demand.

References

[1] M. Malisoff and F. Mazenc, *Constructions of strict Lyapunov functions*. Springer Science & Business Media, 2009.

[2] F. Ghorbel, B. Srinivasan, and M. W. Spong, "On the uniform boundedness of the inertia matrix of serial robot manipulators," *Journal of Robotic Systems*, vol. 15, no. 1, pp. 17–28, 1998.

[3] R. M. Murray, Z. Li, S. S. Sastry, and S. S. Sastry, *A Mathematical Introduction to Robotic Manipulation*. CRC press, 1994.

[4] T. Samad, S. Mastellone, P. Goupil, A. van Delft, A. Serbezov, and K. Brooks, "IFAC industry committee update, initiative to increase industrial participation in the control community," in *Newsletters April 2019*. IFAC, 2019.

[5] K. J. Åström and T. Hägglund, "The future of PID control," *Control engineering practice*, vol. 9, no. 11, pp. 1163–1175, 2001.

[6] P. Shah and S. Agashe, "Review of fractional PID controller," *Mechatronics*, vol. 38, pp. 29–41, 2016.

[7] J. Sánchez, M. Guinaldo, S. Dormido, and A. Visioli, "Validity of continuous tuning rules in event-based pi controllers using symmetric send-on-delta sampling: An experimental approach," *Computers & Chemical Engineering*, p. 106878, 2020.

[8] R. Kelly and R. Carelli, "A class of nonlinear PD-type controllers for robot manipulators," *Journal of Robotic Systems*, vol. 13, no. 12, pp. 793–802, 1996.

[9] A. Haraux and M. A. Jendoubi, *The Convergence Problem for Dissipative Autonomous Systems: Classical Methods and Recent Advances*. Springer, 2015.

[10] S. Kolathaya, "PD tracking for a class of underactuated robotic systems with kinetic symmetry," *IEEE Control Systems Letters*, vol. 5, no. 3, pp. 809–814, 2020.

[11] Q. Chen, H. Chen, Y. Wang, and P.-Y. Woo, "Global stability analysis for some trajectory-tracking control schemes of robotic manipulators," *Journal of Robotic Systems*, vol. 18, no. 2, pp. 69–75, 2001.

[12] T. Ravichandran, D. Wang, and G. Heppler, "Stability and robustness of a class of nonlinear controllers for robot manipulators," in *Proceedings of the 2004 American Control Conference*, vol. 6. IEEE, 2004, pp. 5262–5267.

[13] D. Calzolari, C. Della Santina, and A. Albu-Schäffer, "Exponential convergence rates of nonlinear mechanical systems: The 1-DoF case with configuration-dependent inertia," *IEEE Control Systems Letters*, vol. 5, no. 2, pp. 445–450, 2021.

[14] M. Maggiore and L. Consolini, "Virtual holonomic constraints for Euler–Lagrange systems," *IEEE Transactions on Automatic Control*, vol. 58, no. 4, pp. 1001–1008, 2012.

[15] A. S. Shiriaev, L. B. Freidovich, and M. W. Spong, "Controlled invariants and trajectory planning for underactuated mechanical systems," *IEEE Transactions on Automatic Control*, vol. 59, no. 9, pp. 2555–2561, 2014.

[16] A. Albu-Schaeffer, D. Lakatos, and S. Stramigioli, "One-dimensional solution families of nonlinear systems characterized by scalar functions on riemannian manifolds," *arXiv preprint:1911.01882*, 2019.

[17] A. Albu-Schaeffer and C. Della Santina, "A review on nonlinear modes in conservative mechanical systems," *Annual Reviews in Control*, 2020.

[18] M. P. d. Carmo, *Riemannian Geometry*. Birkhäuser, 1992.

[19] K. Crane, C. Weischedel, and M. Wardetzky, "Geodesics in heat: A new approach to computing distance based on heat flow," *ACM Transactions on Graphics (TOG)*, vol. 32, no. 5, pp. 1–11, 2013.

[20] F. Bullo and A. D. Lewis, *Geometric Control of Mechanical Systems: Modeling, Analysis, and Design for Simple Mechanical Control Systems*. Springer, 2019, vol. 49.

[21] H. K. Khalil, *Nonlinear Systems*. Prentice hall Upper Saddle River, NJ, 2002, vol. 3.

[22] A. Graham, *Nonnegative Matrices and Applicable Topics in Linear Algebra*. Dover Publications, 2019.